Precision Measurements of Atomic Polarizabilities

William Arie van Wijngaarden

Physics and Astronomy Dept.
4700 Keele St., Petrie Bldg., York University
Toronto, Ontario, Canada, M3J 1P3
www@yorku.ca

Abstract. Substantial progress has occurred during the last decade to develop improved methods for determining atomic polarizabilities. We review work that has been done on ground states as well as the study of Stark shifts of transitions to excited states that have been made with a precision of parts in 10^4. Measurements done on alkali atoms have yielded significantly more accurate data than previously available, stringently testing atomic theory.

INTRODUCTION

Polarizabilities describe the response of an atom to a static external electric field and are essential to determine a wide variety of quantities including charge exchange cross sections, van der Waals constants, dielectric constants, indices of refraction, electric fields in plasmas, etc. [1,2]. It is surprising that the polarizabilities of most elements have not been measured and few have been precisely determined. Several review articles describing various techniques to measure polarizabilities have been written including ones by Miller and Bederson [3,4] that describe the study of atoms and molecules and a text by Bonin and Kresin that discusses work done on clusters [5].

During the last decade, several groups have developed techniques that have determined atomic polarizabilities of alkali atoms with accuracies as high as parts in 10^4 [6-10]. This represents an improvement in accuracy of more than two orders of magnitude. Hence, measured polarizabilities provide a stringent test of atomic theory. Work has been done on ground states as well as on excited states that have been studied by precisely measuring Stark shifts of transition frequencies. Alkali atoms are of particular interest to theorists as they possess only a single valence electron and can therefore be relatively easily modeled. Applications of alkali atoms include atomic clocks [11], Bose-Einstein condensation [12] and parity-violation experiments [13,14].

CP477, *Atomic Physics 16*, edited by W. E. Baylis and G. W. F. Drake

This article briefly reviews some of the newly developed techniques to measure polarizabilities and discuss their results. This paper is organized as follows. First, the definitions of polarizabilities are stated and work studying the ground state is reviewed. This is followed by a presentation of optical techniques to accurately measure Stark shifts of alkali D lines as well as transitions to Rydberg states. Finally, conclusions are discussed.

DEFINITION OF POLARIZABILITIES

An external electric field $\mathbf{E}$ polarizes the electron cloud of an atom shifting the energy of an atomic state ψ. The first order shift is given by $\langle\psi|e\mathbf{E}\cdot\mathbf{r}|\psi\rangle$ where e is the electron charge and $\mathbf{r}$ is the electron position vector. This matrix element vanishes for atomic states of alkali atoms which have a definite parity. Hence, in general the Stark shift is second order in the electric field and is given by the following Hamiltonian [15].

$$H_{Stark} = -\Big\{\alpha_0 + \alpha_2 \frac{3J_z^2 - \mathbf{J^2}}{J(2J-1)}\Big\}\frac{E^2}{2} \tag{1}$$

Here, $\mathbf{J}$ is the total electronic angular momentum of the state and J_z is the operator along the quantized direction z specified by the electric field direction. The second term is absent when $J = 0, 1/2$. The scalar α_0 and tensor α_2 polarizabilities are given by

$$\alpha_0 = \frac{r_o}{4\pi^2}\sum_{J'}\lambda_{JJ'}^2 f_{JJ'} \tag{2}$$

$$\alpha_2 = \frac{r_o}{8\pi^2}\frac{1}{(2J+3)(J+1)}\sum_{J'}\lambda_{JJ'}^2 f_{JJ'}[8J(J+1) - 3X(X+1)] \tag{3}$$

where $X = J'(J'+1) - J(J+1) - 2$, r_o is the classical electron radius, $\lambda_{JJ'}$ is the wavelength for a transition between states J and J', and $f_{JJ'}$ is the oscillator strength. The eigenstates of the Hamiltonian are $|Jm_J\rangle$ where m_J is the azimuthal quantum number and the corresponding eigenenergy is given by

$$E_{Jm_J} = -\Big\{\alpha_0 + \alpha_2 \frac{3m_J^2 - J(J+1)}{J(2J-1)}\Big\}\frac{E^2}{2}. \tag{4}$$

The scalar and tensor polarizabilities have units of length cubed. Convenient atomic units are $a_o^3 = 1.4818\times10^{-25}$ cm^3 where a_o is the Bohr radius. Alternatively, polarizabilities can be expressed in terms of the frequency shift produced by an electric field, i. e. 1 kHz/(kV/cm)^2 $= 4.0189a_o^3/h$ where h is Planck's constant. Polarizabilities strongly depend on the electron position and are proportional to n^7 where n is the principal quantum number [16]. Hence, excited states have much larger polarizabilities than do ground states.

GROUND STATE POLARIZABILITIES

The earliest work studied ground states by passing an atomic beam through an inhomogeneous electric field [17]. The atoms experienced a force $\mathbf{F} = \alpha_0 \nabla(E^2/2)$ in the direction transverse to their velocity. The deflection of the atoms was measured using a hot wire detector which ionized the atoms and measured the resulting current. This method determined the alkali ground state polarizabilities to about 10% accuracy. The uncertainty arises principally from the determination of the electric field gradient which is calculated from the electrode geometry. Another complication is the spread of atomic velocities which broadens the spatial profile of the deflected beam. Later versions of the experiment used a velocity selector and obtained a result of $\alpha_0 = 41.0 \pm 2.9$ kHz/(kV/cm)^2 for the sodium ground state [18].

The so called E-H gradient balance, developed by Bederson et al. [19], was much less sensitive to the distribution of atomic velocities. The electrodes used to generate the electric field gradient also served as the pole pieces of a Stern Gerlach inhomogeneous magnetic field dH/dz. Atoms were not deflected if the electric and magnetic forces canceled i.e. $\alpha(m_J)EdE/dz = \mu(m_J)dH/dz$ where μ_J is the magnetic moment. This force cancellation is independent of the atom's velocity. Hence, this method had a larger signal to noise ratio than the earlier technique. The accuracy was limited by the determination of the electric field gradient which was found using a beam of metastable helium atoms whose polarizability was known. A value of 39.6 ± 0.8 kHz/(kV/cm)^2 was obtained for the sodium ground state polarizability.

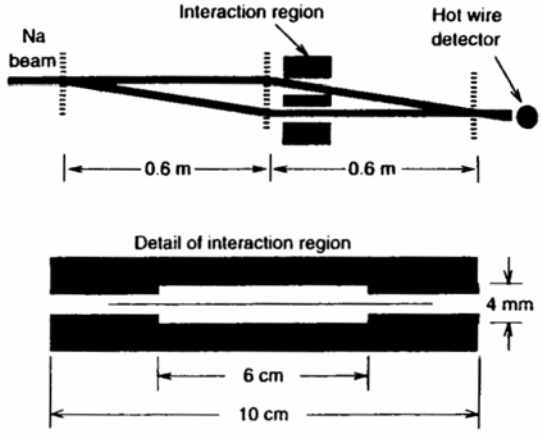

FIGURE 1. Apparatus used to determine ground state polarizability of sodium using atom interferometry. (Reprinted with permission from D. Pritchard [20].)

Recently, a significantly improved value for the ground state sodium polarizability

was obtained using atom interferometry [20]. The apparatus consisted of a three grating Mach-Zender interferometer illustrated in Fig. 1. The transmission gratings had a 200 nm period and generated two atomic beams separated by 55 μm. One beam passed through an electric field created by applying a voltage across two metal foils which generated a relative phase shift between the two atomic beams given by

$$\Delta\phi = \frac{1}{\hbar v}\int_0^L \frac{\alpha_0 E^2}{2} dx. \tag{5}$$

Here v is the velocity of the atoms, α_0 is the ground state polarizability, E is the electric field and L is the length of the electric field region. The two beams were recombined and the resulting interference pattern was studied using a movable hot wire detector. Phase shifts of up to 60 rad were observed using fields of several kV/cm and α_0 was determined to be 40.56 ± 0.14 kHz/(kV/cm)^2. The uncertainty is due to statistical and systematic effects. The latter is dominated by geometrical effects such as fringing electric fields that affect the interaction length L. Another complication was modeling the velocity distribution of the atoms in the atomic beam to estimate the average velocity.

POLARIZABILITIES OF FIRST EXCITED STATES

The methods used to determine polarizabilities of ground states are not applicable to study excited states that have short radiative lifetimes. Several techniques exist to determine excited state polarizabilities including optical double resonance [21] and quantum beat spectroscopy [22]. We shall describe how more accurate data has been obtained by measuring Stark shifts.

An electric field shifts a transition frequency by an amount

$$\Delta\nu = \frac{K}{2}E^2. \tag{6}$$

The Stark shift rate, K, depends on the polarizabilities of the upper and lower states of the transition. For a $S_{1/2} \rightarrow P_{3/2}$ transition,

$$K = \alpha_0(S_{1/2}) - \alpha_0(P_{3/2}) - \alpha_2(P_{3/2})({m_J}^2 - 5/4). \tag{7}$$

A typical experiment is illustrated in Fig. 2. A laser excites an atomic beam as it passes through a field free region and in an electric field. The laser frequency ν is scanned across the resonance while two detectors (Det 1 & 2) monitor fluorescence produced by the radiative decay of the excited atoms. The change in laser frequency is found using a Fabry-Perot interferometer that transmits light whenever the laser frequency changes by a free spectral range $\nu_{\rm FSR} = c/2nL$, where c is the speed of light, n is the index of refraction of the air occupying the cavity and L is the etalon length. This method has been used to study a number of transitions,

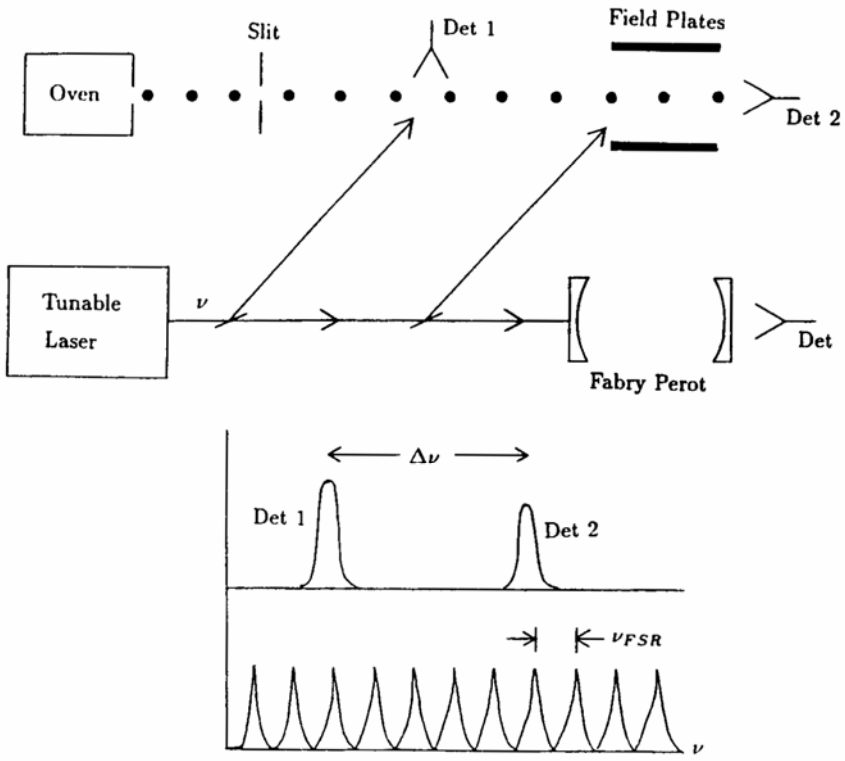

FIGURE 2. Typical apparatus used to measure Stark shifts using a Fabry-Perot interferometer to calibrate frequency.

including the sodium D lines [7]. The frequency calibration is limited by vibrations of the cavity and pressure/temperature fluctuations that perturb the refractive index n. These problems are reduced by using a HeNe laser that is locked to an iodine transition to stabilize the etalon length and enclosing the interferometer in a vacuum chamber [10]. This paper focuses on techniques that determine frequency shifts more accurately and conveniently.

Tanner and Wieman studied the cesium $6S_{1/2} \rightarrow 6P_{3/2}$ transition using the apparatus illustrated in Fig. 3 [6]. A diode laser at 852 nm was locked to the transition observed using saturation spectroscopy in a cell while an acousto-optic modulator (AO) frequency shifted part of the laser beam into resonance with atoms experiencing an electric field. This permitted the determination of $\alpha_0(6P_{3/2}) - \alpha_0(6S_{1/2}) = 308.6 \pm 0.6$ and $\alpha_2(6P_{3/2}) = -65.3 \pm 0.4$ kHz/(kV/cm)^2. These data agree with values of 308.0 and -65.1 kHz/(kV/cm)^2 computed by Zhou and Norcross using a semiempirical potential composed of a Thomas-Fermi potential plus a term describing the polarization of the inner electron core [23].

Another method to measure Stark shifts is the laser heterodyne technique illustrated in Fig. 4. It was used to study the cesium $6S_{1/2} \rightarrow 6P_{1/2}$ transition [8]. One

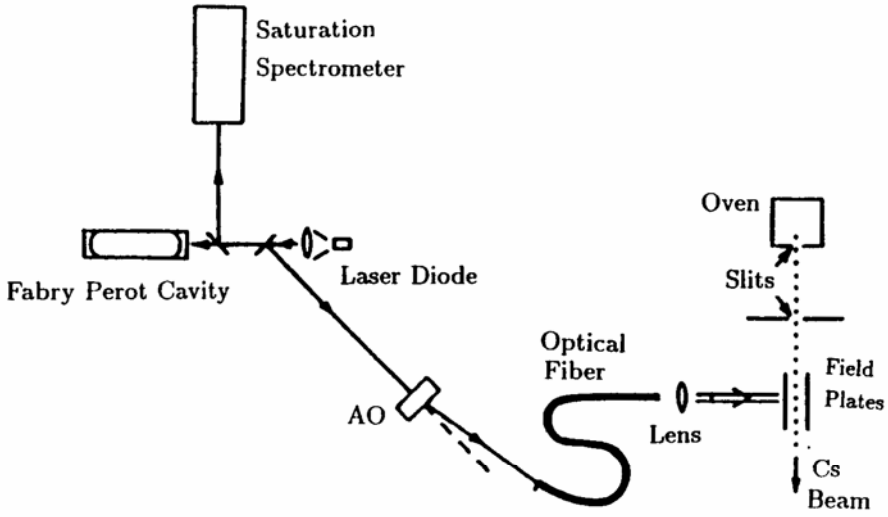

FIGURE 3. Apparatus used to study the cesium $6S_{1/2} \rightarrow 6P_{3/2}$ transition. (Reprinted with permission from C. Tanner [6].)

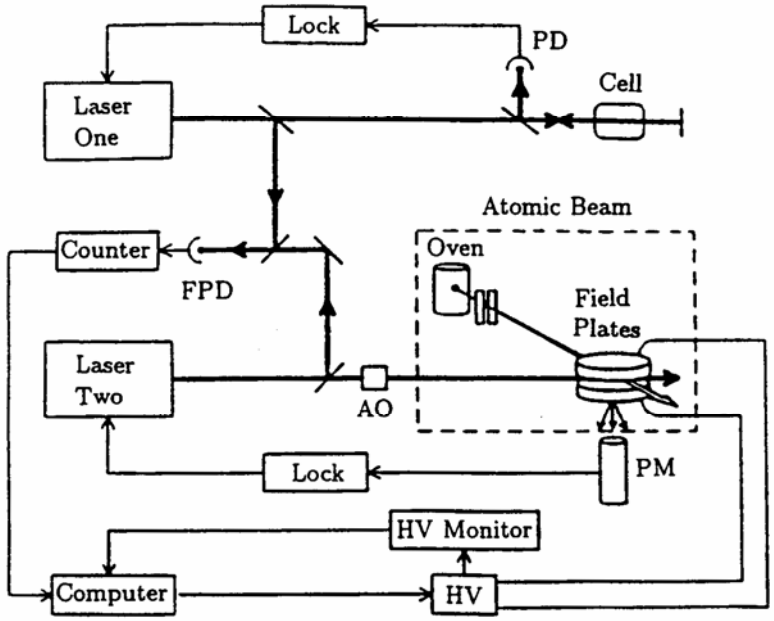

FIGURE 4. Apparatus used to determine Stark shifts of the alkali D lines.

Reprinted from Optics Communications 94, L. R. Hunter et al., Precise measurement of the Stark shift of the cesium D1 line, 210, © 1992, with permission from Elsevier Science.

TABLE 1. Accuracy of the electric-field determination.

Effect	Contribution
Plate Spacing	0.025
Voltage Divider	0.015
Voltmeter	<0.005
Voltage Stability	<0.01
Fringing Field Effects	<0.01
Total Uncertainty	0.029

diode laser was locked to a transition observed in a cesium cell by a photodiode (PD) while a second laser was locked to a Stark shifted transition observed by a photomultiplier (PM). The two laser beams were superimposed onto a fast photodiode (FPD) and a frequency counter measured the beat frequency as a function of the high voltage (HV) applied across the field plates. The latter consisted of two aluminum coated glass plates that formed an etalon. The plate spacing was found using a laser and a wavemeter to measure the etalon's free spectral range. The result of $\alpha_0(6P_{1/2}) - \alpha_0(6S_{1/2}) = 230.44 \pm 0.03$ kHz/(kV/cm)^2 compares to a value of 230.5 kHz/(kV/cm)^2 computed by Zhou and Norcross [23]. The experimental accuracy is limited primarily by uncertainty in the determination of the voltage applied across the field plates.

POLARIZABILITIES OF RYDBERG STATES

Rydberg states can be populated via stepwise excitation using several lasers as is illustrated in Fig. 5. In our experiments, the cesium $6P_{3/2}$ state was excited using a diode laser (SDL 5712-H1) at 852 nm. A ring dye laser (Coherent 699) then excites either a S or D state whose transition wavelength is in the range of 535 to 605 nm, using Pyromethene 556 or Rhodamine 6G laser dyes.

The apparatus is illustrated in Fig. 6. An atomic beam was generated by an oven enclosed in a vacuum chamber that was pumped to a pressure of 2×10^{-7} torr by two diffusion pumps and a liquid nitrogen trap. The atoms were collimated using several slits to produce a beam having a divergence of 1 milliradian. The atomic beam was intersected by laser beams in a region free of electric fields as well as between the two field plates. The latter were made of stainless steel and have a diameter of 12.70 cm. The plate spacing was measured using machinists calibration blocks to be 2.5395 ± 0.0006 cm. Voltages of up to 50 kV can be applied across the plates. The voltage was determined using a voltage divider having an accuracy of 0.015% and a precision voltmeter (HP 34401A). Other effects such as voltage stability of the power supply and fringing fields which were numerically modeled, were negligible as is shown in Table 1.

The diode laser produced about 100 mW of single mode light. Part of this laser beam was passed through a pyrex cell that had been evacuated and loaded with cesium metal. The cesium $6P_{3/2} \rightarrow 6S_{1/2}$ transition excited in a cell has a Doppler

broadened width of about 0.5 GHz as compared to a natural linewidth of 5 MHz when observed using an atomic beam. Hence, the cesium cell was useful to find the transition. Two infrared cameras monitored the fluorescence produced by the radiative decay of the $6P_{3/2}$ state.

The ring dye laser was electronically stabilized and has a manufacturer specified linewidth of 0.5 MHz. The laser beam passed through either an acousto-optic or electro-optic modulator. The modulation signal was supplied by a signal synthesizer (Hewlett Packard 8647A) with an accuracy of one part in 10^6 and amplified to a power of 4 W (Amplifier Research 4W1000). An acousto-optic modulator was used to study the $(10-13)S_{1/2}$ states [9] while an electro-optic modulator was used for the $(10-13)D_{3/2,5/2}$ states [24,25]. In general, acousto-optic modulators operate at lower modulation frequencies. We used an acousto-optic modulator (Brimrose TEF 27-10) that frequency shifted over 50% of the incoming laser light for modulation frequencies in the range of 220–320 MHz. The electro-optic (EO) modulator (ν Focus 4421) shifted over half of the incoming light for modulation frequencies between 995 and 1005 MHz. Electro-optic modulators have the advantage of not spatially deflecting the frequency shifted laser components unlike acousto-optic modulators. This simplifies the alignment of the laser and atomic beams. Precision measurements with acousto-optic modulators have been reviewed [10], and the remainder

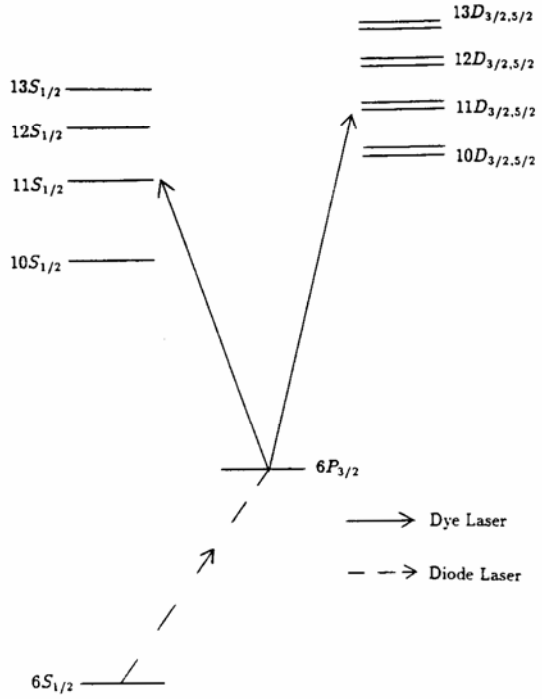

FIGURE 5. Laser excitation of cesium Rydberg states.

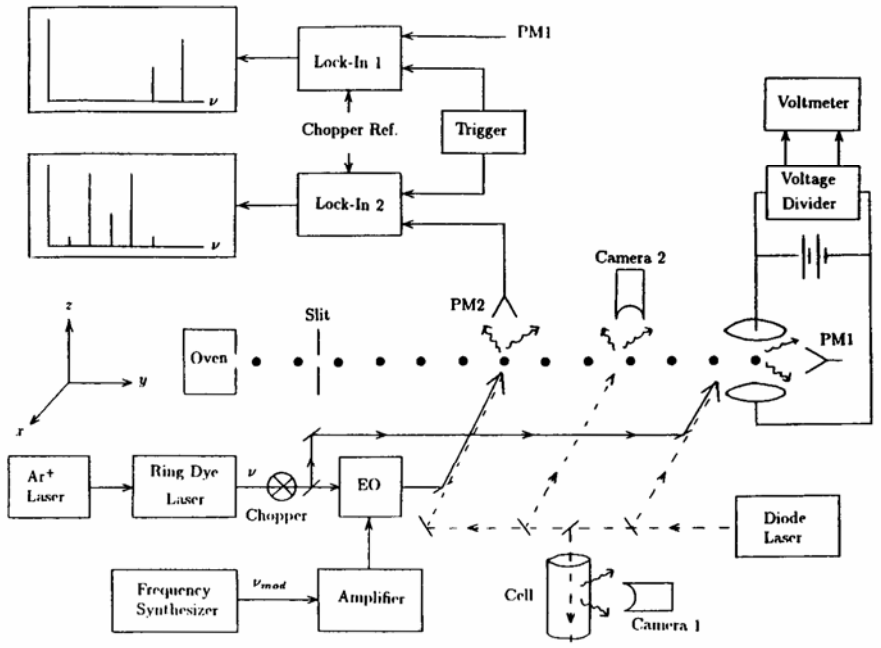

FIGURE 6. Apparatus used to study Stark shifts of cesium $6P_{3/2} \rightarrow (10-13)D_{3/2,5/2}$ transitions.

of this article therefore discusses work done using electro-optic modulators.

The diode and dye laser beams were superimposed and intersected the atomic beam orthogonally to eliminate the first order Doppler shift. Fluorescence, produced by the radiative decay of the excited state, was detected from the field free region and from between the electric field plates by two photomultipliers (Hamamatsu R928). Their signals were processed by two independent lock-in amplifiers (SRS 850) where the reference signal was supplied by a chopper that modulated the dye laser beam at a frequency of 2 kHz. The lock-in amplifiers digitized the demodulated signal when externally triggered by a signal generator at a rate of 256 Hz.

Sample signals are shown in Fig. 7. This scan took about 2 minutes and consisted of approximately 30,000 points. Five peaks are shown in Fig. 7a due to excitation of the $6P_{3/2} \rightarrow 11D_{3/2}$ transition by the laser frequencies ν, $\nu \pm \nu_{\rm mod}$, $\nu \pm 2\nu_{\rm mod}$ where the modulation frequency $\nu_{\rm mod} = 1000.000$ MHz. The number of points separating the various 1 GHz intervals was found using several hundred different scans and were found to be consistent with each other, showing that the frequency scan is linear to better than one part in 1000 [10]. Each point corresponded to an average value of 0.1898 ± 0.0003 MHz.

Data were first taken without any voltage applied to the electric field plates to check whether the atoms in the two regions where the laser intersects the atomic

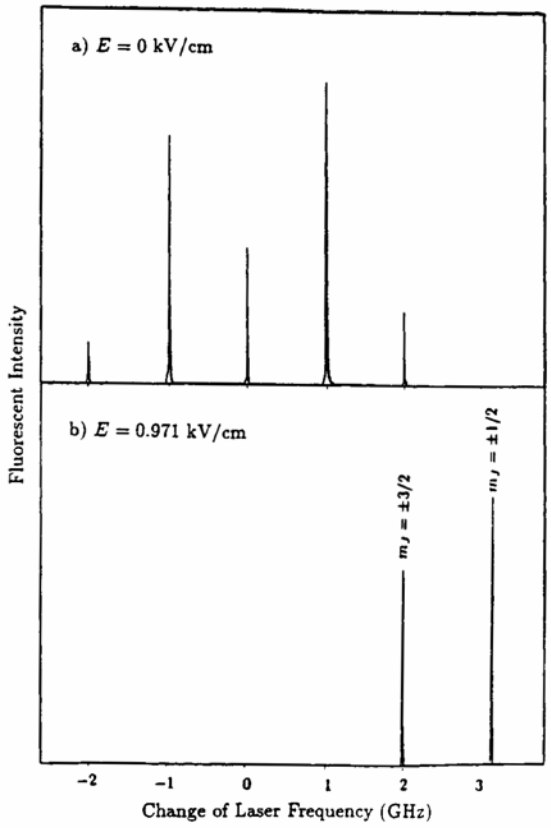

FIGURE 7. Fluorescence versus change of laser frequency. Fig. 7a shows the signal generated when the frequency modulated laser excited the atomic beam in a field-free region, while Fig. 7b shows the signal produced when atoms in an electric field are excited by the unmodulated laser beam.

beam were excited by the same laser frequency. A frequency offset ν_{off} occurs if there is a slightly different alignment of the laser beams in the two regions with the atomic beam creating a different residual first order Doppler shift. ν_{off} was measured to have an average value of 7.97 ± 0.45 MHz.

Data were next taken by applying an electric field across the plates. The dye laser was linearly polarized parallel to the electric field and therefore excited the atoms from the $6P_{3/2}$ state to the $|m_J| = 1/2, 3/2$ levels of the $D_{3/2,5/2}$ states. Hence, the fluorescence signal shown in Fig. 7b shows two peaks. The lock-in amplifier located the peak centers by fitting a Gaussian function to the data. The results were found to be independent of voltage polarity and the dye laser power, which was varied by a factor of 100 using neutral-density filters. The lineshape was broadened at the higher powers but the peak was not frequency shifted. Each dye laser beam was

attenuated to a power of less than 1 mW to reduce power broadening while data such as shown in Fig. 7, were collected.

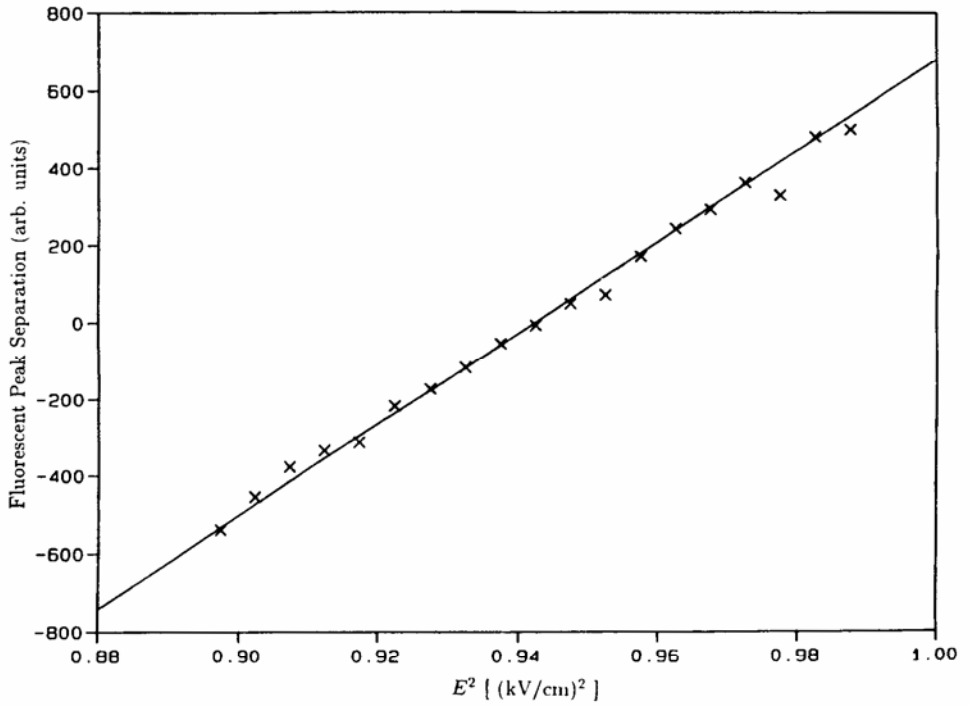

FIGURE 8. Fluorescent peak separation versus electric field squared for the $11D_{5/2}, |m_J| = 3/2$ level.

The Stark Shift rate K was found by measuring the electric field such that the peak observed in the electric field region overlapped with the peak generated by the second laser sideband. The exact field strength was found by plotting the frequency separation of the two peaks versus the square of the electric field as is shown in Fig. 8. The data was fitted to a straight line and a Stark shift of 2000 MHz was found to occur at an electric field of 970.82 ± 0.42 V/cm.

Figure 9 shows data taken when the dye laser excited the $6P_{3/2} \rightarrow 11D_{5/2}$ transition. The frequency shift does not depend quadratically on the electric field due to Stark mixing of the fine structure states which can be seen by diagonalizing the Hamiltonian

$$H = a\mathbf{L} \cdot \mathbf{S} - \left\{\alpha_0 + \alpha_2 \frac{3L_z^2 - \mathbf{L}^2}{L(2L-1)}\right\} \frac{E^2}{2}. \tag{8}$$

The first term is the spin orbit interaction, a is the coupling constant, $\mathbf{L}$ is the orbital electronic angular momentum and $\mathbf{S}$ is the electronic spin. The eigenenergies are plotted in Fig. 10. For weak fields, the Stark shift rate K is

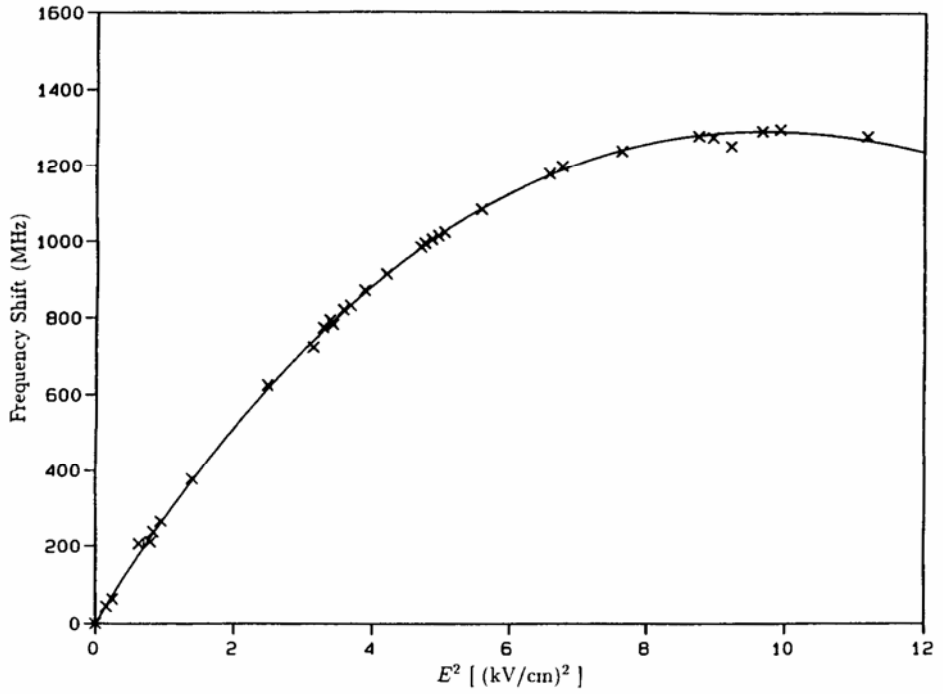

FIGURE 9. Frequency shift versus electric field squared for the $11D_{3/2}, |m_J| = 3/2$ level. The fitted function is given by $y = 293.55E^2 - 19.4E^4 + 0.29E^6$ where y is the frequency shift (MHz) and E is the electric field measured in kV/cm.

$$
\begin{aligned}
K(D_{5/2}, |m_J| = 1/2) &= -\alpha_0(D_{5/2}) + \frac{4}{5}\alpha_2(D_{5/2}) + \frac{3}{250}\frac{\alpha_2(D_{5/2})^2}{a}E^2 \\
K(D_{5/2}, |m_J| = 3/2) &= -\alpha_0(D_{5/2}) + \frac{1}{5}\alpha_2(D_{5/2}) + \frac{9}{125}\frac{\alpha_2(D_{5/2})^2}{a}E^2 \\
K(D_{5/2}, |m_J| = 5/2) &= -\alpha_0(D_{5/2}) - \alpha_2(D_{5/2}) \\
K(D_{3/2}, |m_J| = 1/2) &= -\alpha_0(D_{3/2}) + \alpha_2(D_{3/2}) - \frac{6}{245}\frac{\alpha_2(D_{3/2})^2}{a}E^2 \\
K(D_{3/2}, |m_J| = 3/2) &= -\alpha_0(D_{3/2}) - \alpha_2(D_{3/2}) - \frac{36}{245}\frac{\alpha_2(D_{3/2})^2}{a}E^2.
\end{aligned}
\tag{9}
$$

For the $|m_J| = 3/2$ levels of the $(10-13)D_{3/2}$ state, data was fit to the function $y = a_1E^2 + a_2E^4 + a_3E^6$. Equation (9) shows a_1 can be identified as $-\alpha_0 - \alpha_2$. The uncertainty of this quantity was conservatively estimated by considering the effect of deleting the term proportional to E^6 in the fitting function. For the $|m_J| = 1/2$ $(10-13)D_{3/2}$ states and the $|m_J| = 1/2, 3/2$ levels of the $(10-13)D_{5/2}$ states, a straight line was fit to determine an initial value of the Stark shift rate K_0. Next,

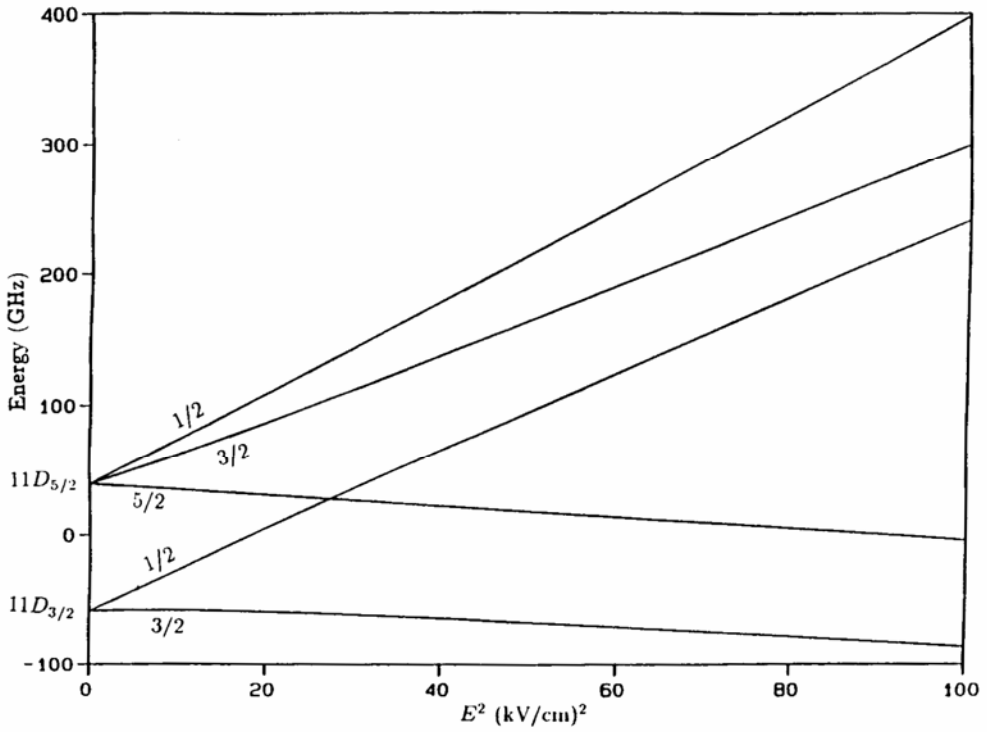

FIGURE 10. Eigenenergies computed for the $11D$ states for the Hamiltonian given in equation 8 using $a = 39.0$ GHz. To first order, the eigenenergies depend quadratically on the electric field. The departure from this quadratic dependence is most noticeable for the $|m_J| = 3/2$ level of the $11D_{3/2}$ state.

the perturbative correction in K quadratic in the field was evaluated. The Stark shift rate was then recalculated and the polarizabilities were obtained as shown in Tables 2 and 3.

Table 3 also lists results obtained by Fredriksson and Svanberg [26]. They used a rf lamp to excite the $6P_{3/2}$ state and a dye laser having a linewidth of 75 MHz to populate the S and D states. Their fluorescent signals had a significantly lower signal to noise ratio than the present work. The change in laser frequency was also determined using an interferometer as illustrated in Fig. 2 while the electric field was determined to an accuracy of a few percent.

The results were also compared to data computed using a so called Coulomb approximation [27,28]. This is a non *ab initio* theoretical model that inputs measured energies into the Schrödinger equation which is then solved using a Coulomb potential to model the interaction between the alkali valence electron with the potential generated by the nucleus and inner electron core. This potential does not include relativistic effects nor the spin orbit interaction which for the $10D_{3/2,5/2}$

TABLE 2. Determination of the Stark shift rate. Units are MHz/(kV/cm)^2.

State	$\lvert m_J \rvert$	K_0	Correction	K
$10D_{3/2}$	1/2	1886.5 ± 1.4	0.66 ± 0.01	1887.5 ± 1.4
	3/2	195.0 ± 1.0		
$10D_{5/2}$	1/2	2677.0 ± 2.6	−0.90 ± 0.01	2676.1 ± 2.6
	3/2	1667.4 ± 1.4	−8.71 ± 0.09	1658.7 ± 1.4
$11D_{3/2}$	1/2	4799.7 ± 4.6	+2.33 ± 0.02	4802.1 ± 4.6
	3/2	587.1 ± 5.8		
$11D_{5/2}$	1/2	6777.4 ± 5.7	−3.21 ± 0.03	6774.2 ± 5.7
	3/2	4259.6 ± 3.8	−30.7 ± 0.3	4229.0 ± 3.8
$12D_{3/2}$	1/2	10864.7 ± 6.4	7.10 ± 0.07	10871.8 ± 6.4
	3/2	1488.6 ± 7.6		
$13D_{5/2}$	1/2	31553 ± 24	−27.0 ± 0.3	31526 ± 24
	3/2	20137 ± 17	−254.1 ± 2.5	19882 ± 18

states is 140 GHz. It is therefore surprising that the calculated polarizabilities are within 1% of the experimental results. Similar agreement between experimental and theoretically determined polarizabilities has been found for the other alkali atoms [29-31]. Clearly, more elaborate theoretical models such as many body perturbation theory [32,33] that take into account effects of polarization of the inner electron core, electron correlation, relativistic corrections can be expected to yield more accurate polarizability values.

CONCLUSIONS

Techniques that determine scalar and tensor polarizabilities with accuracies of one part in a thousand or higher have been demonstrated in the last decade. Atom interferometry is especially well suited to study ground states as was demonstrated for sodium. Polarizabilities of excited states can be found by measuring Stark shifts of optical transitions. The laser heterodyne technique is attractive to study first excited states that can be populated using relatively inexpensive diode lasers. Hunter et al used this method to investigate Stark shifts of D lines of several alkali atoms [10]. In general, transitions whose wavelengths are inaccessible to diode lasers, including ones to Rydberg states, can be studied using acousto/electro optical modulators to precisely determine Stark shifts.

The measurements challenge our theoretical understanding of many electron atoms. The polarizabilities computed using the simple Coulomb approximation were found to be within 1% of the experimental data. It is however essential to take into account Stark induced mixing of the fine structure states. Improved agreement between theory and experiment is likely to result from more elaborate calculations as discussed previously. Existing theoretical work has been largely

TABLE 3. Polarizabilities of some cesium Rydberg states. Units are MHz/(kV/cm)^2.

State	α_0	α_2	Ref.
$10S_{1/2}$	123 ± 6		26
	119.06 ± 0.28		9
	118		27
$11S_{1/2}$	322 ± 16		26
	309.70 ± 0.26		9
	309		27
$12S_{1/2}$	720 ± 45		26
	713.48 ± 0.58		9
	709		27
$13S_{1/2}$	1650 ± 170		26
	1491.2 ± 1.2		9
	1490		27
$10D_{3/2}$	-1150 ± 170	840 ± 40	26
	-1041.3 ± 0.9	846.3 ± 0.9	25
	-1050	848	27
$11D_{3/2}$	-2694.6 ± 2.7	2107.5 ± 2.7	24
	-2712	2120	27
$12D_{3/2}$	-6180.0 ± 4.9	4691.4 ± 4.9	25
	-6245	4753	27
$13D_{3/2}$	-12935 ± 18	9620 ± 18	25
	-12989	9679	27
$10D_{5/2}$	-1340 ± 130	1770 ± 90	26
	-1319.5 ± 2.1	1695.7 ± 4.9	25
	-1319	1704	27
$11D_{5/2}$	-3790 ± 350	4010 ± 400	26
	-3379.5 ± 5.4	4242 ± 11	24
	-3384	4255	27
$12D_{5/2}$	-7660 ± 15	9501 ± 39	25
	-7738	9530	27
$13D_{5/2}$		19000 ± 1000	26
	-16001 ± 25	19406 ± 49	25
	-16099	19533	27

confined to the cesium D lines which are of importance for tests of parity violation.

The work discussed in this paper is readily applicable to other atomic systems. It should be relatively straight forward to apply the atom interferometric method to study ground states of other alkali atoms. Similarly, Stark shifts have only been investigated for a small number of transitions in alkali and alkaline-earth atoms [10]. These experimental results complement information about of atomic wavefunctions obtained by measurements of radiative lifetimes [34] and oscillator strengths [35]. Polarizabilities can however be determined with much higher precision. Hence, precision measurements of polarizabilities will be of continued future interest for investigating atomic structure.

ACKNOWLEDGMENTS

This work was supported by the Natural Sciences and Engineering Research Council of Canada and York University. We would like to thank J. Clarke for proof reading the manuscript.

REFERENCES

1. Kadar-Kallen, M. A., and Bonin, K. D., *Phys. Rev. Lett.* **72**, 828 (1994).
2. Lawler, J. E., and Doughty, D. A., *Adv. At. Mol. Phys.* **34**, 171 (1995).
3. Miller, T. M., and Bederson, B., *Adv. At. Mol. Opt. Phys.* **13**, 1 (1977).
4. Miller, T. M., and Bederson, B., *Adv. At. Mol. Opt. Phys.* **25**, 37 (1988).
5. Bonin, K. D., and Kresin, V., *Electric Dipole Polarizabilities of Atoms, Molecules and Clusters*, Singapore: World Scientific Press, 1997.
6. Tanner, C. E., and Wieman, C., *Phys. Rev. A* **38**, 162 (1988).
7. Windholz, L., Musso, M., *Phys. Rev. A* **39**, 2472 (1989).
8. Hunter, L. R., Krause, D., Miller, K. E., Berkeland, D. J. and Boshier, M. G., *Opt. Commun.* **94**, 210 (1992).
9. van Wijngaarden, W. A., Hessels, E. A., Li, J., and Rothery, N. E., *Phys. Rev. A* **49**, R2220 (1994).
10. van Wijngaarden, W. A., *Adv. At. Mol. Opt. Phys.* **36**, 141 (1996).
11. Itano, W. M., Lewis, L. L., and Wineland, D. J., *J. de Physique* **42**, 283 (1981).
12. Anderson, M. H., Ensher, J. R., Matthews, M. R., Wieman, C. E., and Cornell, E. A., *Science*, **269**, 198 (1995).
13. Wood, C. S., Bennett, S. C., Cho, D., Masterson, B. P., Roberts, J. L., Tanner, C. E., and Wieman, C. E., *Science* **275**, 1759 (1997).
14. Dzuba, V. A., Flambaum, V. V., and Sushkov, O. P., *Phys. Rev. A* **51**, 3454 (1995).
15. Khadjavi, A., Lurio, A., and Happer, W., *Phys. Rev.* **167**, 128 (1968).
16. Bethe, H. A., and Salpeter, E. E., *Quantum Mechanics of One and Two Electron Atoms*, New York: Plenum Press, 1977.
17. Chamberlain, G. E., and Zorn, J. C., *Phys. Rev.* **129**, 677 (1963).
18. Hall, W. D., and Zorn, J. C., *Phys. Rev. A* **10**, 1141 (1974).

19. Molof, R. W., Schwartz, H. L., Miller, T. M., and Bederson, B., *Phys. Rev. A* **10**, 1131 (1974).
20. Ekstrom, C. R., Schmiedmayer, J., Chapman, M. S., Hammond, T.D., and Pritchard, D. E., *Phys. Rev. A* **51**, 3883 (1995).
21. Rinkleff, R. H., *Z. Phys. A* **296**, 101 (1980).
22. Kulina, P., and Rinkleff, R. H. *Z. Phys. A* **304**, 371 (1982).
23. Zhou, H. L, and Norcross, D. W., *Phys. Rev. A* **40**, 5048 (1989).
24. van Wijngaarden, W. A., and Li, J., *Phys. Rev. A* **55**, 2711 (1997).
25. Xia, J., Clarke, J., Li, J., and van Wijngaarden, W. A., *Phys. Rev. A* **56**, 5176 (1997).
26. Fredriksson, K., and Svanberg, S., *Z. Phys. A* **281**, 189 (1977).
27. van Wijngaarden, W. A., and Li, J., *J. Quant. Spectrosc. Radiat. Transfer* **52**, 555 (1994).
28. Bates, D. R., and Damgaard, A., *Philos. Trans. R. Soc. London* **242**, 101 (1949).
29. Gruzdev, P. F., Soloveva, G. W., and Sherstyuk, A. I., *Opt. Spectrosc.* **71**, 513 (1991).
30. van Wijngaarden, W. A., *J. Quant. Spectrosc. Radiat. Transfer* **57**, 275 (1997).
31. van Wijngaarden, W. A., and Xia, J., *J. Quant. Spectrosc. Radiat. Transfer* in press (1998).
32. Dzuba, V. A., Flambaum, V. V., Silvestrov, P. G., and Sushkov, O. P., *Phys. Lett. A* **140**, 493 (1989).
33. Blundell, S. A., Johnson, W. R., and Sapirstein, J., *Phys. Rev. A* **43**, 3407 (1991).
34. Rafac, R. J., Tanner, C. E., Livingtston, A. E., Kukla, K. W., Berry, H. G. and Kurtz, C. A., *Phys. Rev. A* **50**, R1976 (1994).
35. van Wijngaarden, W. A., Bonin, K. D., Happer, W., Miron, E., Schreiber, D., and Arisawa, T., *Phys. Rev. Lett.* **56**, 2024 (1986).